

Simulations of PEFC cathodes: an effectiveness factor approach

F. GLOAGUEN*

Electrochimie et Interactions, 40 av. du Recteur Pineau, 86022 Poitiers, France

R. DURAND

LEPMI, BP 75, 38402 St Martin d'Hères, France

Received 9 September 1996; revised 4 November 1996

The key parameters describing the operation mechanism of an active layer of PEFC cathodes were discussed. The macrohomogeneous and the agglomerate model were applied to different kinds of oxygen cathodes. From the simulations, it appears that gas pores must exist, even within real active layers thinner than 10 μm . The more appropriate model is the agglomerate model. An effectiveness factor approach allowed determination of the main factors limiting the oxygen cathode performance. Actual solutions for further improvements of the catalyst utilization were derived from simulations.

1. Introduction

Simulation of porous electrode performances is important for design purposes, as well as for the determination of limiting factors. In fuel cell (FC) systems using a proton exchange (PE) polymer as electrolyte, the porous electrodes are usually formed by a gas diffusion layer holding an active layer. The latter consists of supported catalyst (e.g., Pt/C) and a recast PE polymer (e.g., recast Nafion[®]). Generally, the active layer also contains some PTFE, e.g. [1]; however, new fabrication methods have recently been reported [2], where PTFE is not used.

As a first approach, the limitation by mass transport through the diffusion layer is usually assumed to be negligible [3]. The electrode polarization characteristics depend mainly on the rate of phenomena occurring inside the active layer, (i) gas diffusion from the diffusion/active layer interface to catalytic sites, (ii) charge transfer across the catalyst/electrolyte interface and (iii) ionic conduction. Various models have been devoted to the operation mechanism of active layers. These models, the simple pore [3], the thin film [4] and the agglomerate [5] model, were first developed for FC systems using a liquid electrolyte. However, polarization characteristics of PEFC electrodes have been recently simulated using the macrohomogeneous model [6, 7] or the filmed agglomerate model [8, 9].

The purpose of the present paper is to compare the macrohomogeneous model and the agglomerate model for the simulations of PEFC cathodes. The key parameters describing the operation mechanism of an active layer are first discussed. Modelling is carried out using an effectiveness factor approach [10]. To

validate this mathematical analysis, the computer generated data are compared to experimental data from recently published results [1, 2]. Fitting to experimental data allows determination of the more suitable model, as well as factors limiting the oxygen cathode performance. Actual solutions for further improvements of the polarization characteristics are obtained.

2. Operation mechanism of an active layer

Calculation of potential and concentration distributions through a porous electrode (e.g., a PEFC active layer) implies knowledge of transport and kinetic parameters. In addition, the use of structural parameters is needed to characterize the electrode geometry.

2.1. Transport parameters

The effective transport parameters within a porous electrode, for example, the diffusion coefficient (D) and the ionic conductivity (σ), are usually estimated from their respective values in bulk media, the volume fraction (θ) of electrolyte and the tortuosity factor (τ). Hence [11]

$$D/D_b = \sigma/\sigma_b = \theta/\tau \quad (1)$$

In the case of PEFC active layers, the volume fraction of Nafion[®] (which is a solid electrolyte) is easy to measure and/or to calculate. Unfortunately, an estimation of the tortuosity factor is much more difficult. As a result, the empirical Bruggeman relationship [11] is preferably used

$$D/D_b = \sigma/\sigma_b = \theta^{3/2} \quad (2)$$

To reduce the number of variables in the simulations, the parameters $D_b c_b$ (c_b being the solubility of

* Author to whom correspondence should be addressed.

oxygen) and σ_b have the same value for FC operating temperatures (T) ranging from 20 to 80 °C. The error introduced in the simulations is difficult to estimate accurately, but the temperature effect should be poor as compared to the influence of the humidity degree [20, 26]. As base-case conditions (Table 1), we use the values for $D_b c_b$ and σ_b , that were measured at room temperature using electrodes coated with recast Nafion® [13, 20, 21]. Since these values of transport parameters were obtained with recast film immersed in water, they are considered here as maximum values.

2.2. Kinetic parameters

To overcome the problem related to the well-known change of Tafel slope (from b about 0.07 to 0.12 V dec⁻¹ at $E \simeq 0.8$ V vs RHE), the kinetics of the oxygen reduction reaction (ORR) are described by [7]

$$i^* = -nFk \exp(-2.3(E - E^\circ)/b) \quad 0.9 \text{ V} > E > 0.7 \text{ V} \quad (3)$$

$i^*(<0)$ is the current density per real catalyst area generated under kinetic control, and k the rate constant of the charge transfer at $E^\circ = 0.9$ V vs RHE (E being the potential of the oxygen cathode). The kinetic parameters k and b can be estimated from previous ORR measurements at a model active layer of well-defined geometry [12]. These measurements were performed at 1 atm and 20 °C using a rotating disc electrode (RDE) coated with Pt/C plus recast Nafion® (e.g., see Fig. 1). Increase of the rate of charge transfer, at a FC operating temperature $T > 20$ °C, is simulated by $k \times \Gamma$, Γ being a temperature parameter. No modifications with temperature of the Tafel slope is accounted for, because b is not always directly proportional to T . In fact, $2.3/b = \alpha z F / RT$, but the transfer coefficient (α) may also be a function of T .

Several publications [e.g. 13–17], have dealt with the measurements of ORR kinetics at the Pt/recast Nafion® interface. These experiments were nevertheless performed using bulk Pt electrodes but Pt/C powders do not have the same catalytic activity as bulk Pt [18, 19].

Table 1. Base-case parameters and cathode properties

	Cathode 1	Cathode 2	Ref
$D_b c_b \times 10^{12} / \text{mol cm}^{-1} \text{s}^{-1}$	12	12	[13, 20]
$\sigma_b / \text{S cm}^{-1}$	0.050	0.015*	[21]
$nFk \times 10^6 / \text{A cm}^{-2}$	12.2	12.2	Fig. 1, [12]
$b / \text{V dec}^{-1}$	0.084	0.084	Fig. 1, [12]
$W \times 10^3 / \text{g cm}^{-2}$	0.35	0.17	[1, 2]
$S \times 10^4 / \text{cm}^2 \text{g}^{-1}$	85	85	[19]
$\rho / \text{g cm}^{-3}$	2.2	2.2	–
m	0.2	0.2	–
Γ	3*	6*	–
$a \times 10^4 / \text{cm}$	1.5*	0.4*	–
β	0.4*	0.1*	–

* Best-fit values calculated using the agglomerate model.

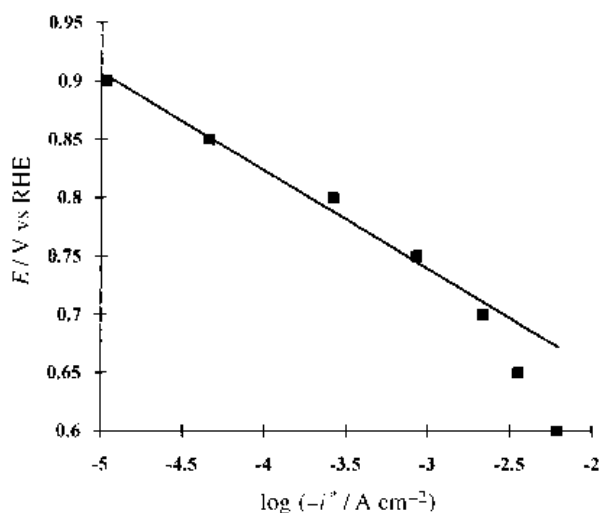


Fig. 1. ORR Tafel plot (from RDE measurements [12]) for a Pt/C plus recast Nafion® electrode at 20 °C and 1 atm. The catalytic powder is a 20 wt % Pt/C from E-TEK. The current density (i^*) is quoted to the real Pt surface area. Two Tafel slopes are visible but for the simulations, the kinetic parameters are extrapolated from a linear regression between 0.9 and 0.7 V.

2.3. Structural parameters

Diffusion and consumption of the reactant through a porous electrode occur simultaneously. The kinetic rate per volume unit is hence $i^* \gamma$, where γ is the surface to volume ratio of catalyst. This indirect structural parameter is calculated as follows:

$$\gamma = (1 - \theta) \rho m S \quad (4)$$

where ρ , m and S are the density of the catalyst powder, the mass fraction of catalyst and its specific area, respectively.

Concerning the operation mechanism of an active layer, it may be assumed that oxygen diffuses from the diffusion/active layer interface towards the catalytic sites either in the electrolyte phase only, or first through gas pores and second within electrolyte. Both hypotheses have to be investigated using an appropriate model, namely the macrohomogeneous or the agglomerate model.

On the one hand, as shown in Fig. 2(a), the macrohomogeneous model assumes that the catalytic sites and the electrolyte are uniformly distributed in volume. The catalyst loading (W) and the layer thickness (L) are therefore related by

$$W = (1 - \theta) \rho m L \quad (5)$$

From this equation, it is clear that knowledge of W and θ (which are experimental data) allows calculation of L for any given catalyst powder.

On the other hand, as shown in Fig. 2(b), the agglomerate model splits the porous electrode into a number of micro- and macroporous regions. The catalyst powder forms microporous agglomerate flooded with electrolyte. Between these agglomerates, a network of electrolyte-free macropores exists, where gas flows quickly [5]. Hence,

$$W = (1 - \beta) (1 - \theta) \rho m L \quad (6)$$

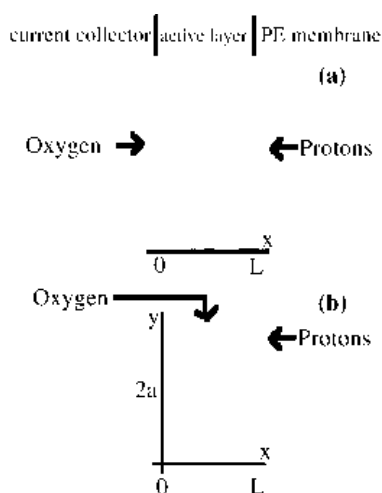


Fig. 2. (a) macrohomogeneous model and (b) agglomerate model as used in the mathematical analysis of PEFC active layers.

β being the volume fraction of gas pores (the macro-porosity). In addition, the use of the agglomerate model implies determination of the agglomerate size a . Unfortunately, experimental measurements of parameters β and a are difficult under FC operating conditions.

3. Mathematical modelling: an effectiveness factor approach

The catalyst utilization appears the most interesting quantity to compare active layers, as well as to visualize the effect of key parameters on the calculated polarization characteristics. As a result, an effectiveness factor (ε) is defined [10]

$$\varepsilon = \text{actual c.d.} / (\text{c.d. without limitation by diffusion and by ohmic drop})$$

and a functional dependence is anticipated, as follows $\varepsilon = f(D_b c_b, \sigma_b, \theta, k, b, W, S, \Gamma, a, \beta)$. At low limitation by diffusion and/or ohmic drop, ε is close to unity, and the catalyst works uniformly through the porous electrode.

To calculate the ε against E curves, $D_b c_b$, σ_b , nFk and b are fixed at values thought to be realistic for PEFC cathodes working at 20 °C and 1 atm (Table 1). The parameters Γ or the set of parameters Γ , a and β were used as variables for the macrohomogeneous model or the agglomerate model, respectively (cf. Appendix). Realistic values of these parameters (Γ , a , β) should be calculated from fitting.

Two kinds of PEFC active layers [1, 2], working as oxygen cathodes, are used to validate the modelling approach. They will be referred as cathode 1 or 2 in the following discussion (Table 1). Cathode 1 is the active layer of a Nafion® impregnated (4 wt%) E-TEK electrode, it therefore contains PTFE (about 40wt%). Cathode 2 consists of Pt/C plus recast Nafion® only. In both cases, the catalyst powder is a 20 wt% Pt/C from E-TEK. The respective polarization characteristics of these cathodes can therefore be

compared without accounting for the particle size effect on the ORR kinetics [19].

The experimental curves to be fitted are extrapolated from those obtained at complete H_2/O_2 PEFC working at 1 atm and 50 °C [1] or 80 °C [2]. At high single cell voltage ($V_{\text{cell}} > 0.7$ V), the hydrogen anode overpotential is neglected [7]. The ohmic drop within the PE membrane is corrected according to $E = V_{\text{cell}} - jR_{\text{HF}}$ with $R_{\text{HF}} = 0.4 \Omega \text{ cm}^{-2}$ [1] or $0.1 \Omega \text{ cm}^{-2}$ [2]. The variation of R_{HF} with current density was not reported in [1]. However, since the generated current densities were rather low, the error introduced in our simulations by using a constant membrane resistance should not be too large, although difficult to estimate. Concerning cathode 2, a rather constant ohmic drop through the membrane was measured up to 1 A cm^{-2} [7].

4. Results and discussion

4.1. Macrohomogeneous model

The macrohomogeneous model is not used to simulate active layers containing PTFE, such as cathode 1. PTFE is supposed to create macropores free of electrolyte where the gas flows quickly. This therefore disagrees with the assumption of a uniform distribution in volume of electrolyte within the active layer.

The current densities calculated by the model are low compared to those actually generated by cathode 2 (Fig. 3). As a result, very fast rates of charge

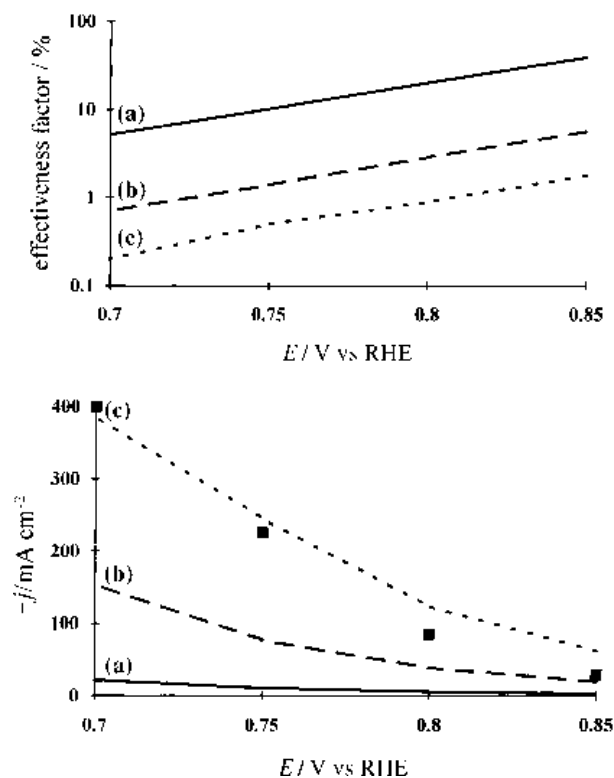


Fig. 3. Simulated curves using the macrohomogeneous model at base-case conditions (see Table 1). Effectiveness factor (ε) and current density (j) are plotted against cathode potential (E). (a) $\Gamma = 1$, (b) = 50, (c) = 500. The squares correspond to experimental data reported in [2].

transfer ($\Gamma = 500$) are required, and the fit is not good. This likely indicates that limitation by oxygen diffusion is overestimated; therefore the calculated values for the catalyst utilization are much too low. In other words, oxygen must diffuse, not only within electrolyte, but also through gas pores. Hence, the macrohomogeneous model seems not suitable to simulate the operation mechanism of any real PEFC cathodes. (This model can nevertheless be used in the case of totally flooded thin layers deposited on a RDE, as reported in [12]). However, as several simulations of real PEFC systems have been recently carried out using the macrohomogeneous model [6, 7], some items must be clarified.

On the one hand, Bernadi *et al.* [6] reported a model simulating a complete PEFC (including the membrane properties), and based on the macrohomogeneous model. In the course of fitting many parameters were adjusted (particularly the product $\gamma \times nFk$ for the cathode). Oxygen permeability in agreement with that experimentally measured in recast Nafion[®] film ($D_b c_b \times \theta^{3/2} \sim 10^{-12} \text{ mol}^{-1} \text{ cm}^{-1} \text{ s}^{-1}$) was also used. As a result, the authors [6] calculated a very low catalyst utilization even at modest current densities (e.g., $\varepsilon < 15\%$ at $j \sim 10 \text{ mA cm}^{-2}$). In spite of the low level of catalyst utilization assumed in [6], current densities higher than 100 mA cm^{-2} were calculated using very high rate of charge transfer for ORR. This agrees with our own calculations using the same model (Fig. 3), but this procedure has no experimental basis. $\Gamma = 500$ corresponds to an activation energy of about 90 kJ mol^{-1} , at least twice the usually reported value. To our understanding, if excessive and, thus, unrealistic values of the rate of charge transfer are required, this simply means that the macrohomogeneous model cannot simulate any real active layer of PEFC, assuming that oxygen diffuses within the electrolyte phase only.

On the other hand, Springer *et al.* [7] assumed oxygen permeability as high as $D_b c_b \times \theta^{3/2} \sim 10^{-9} \text{ mol cm}^{-1} \text{ s}^{-1}$, caused by oxygen diffusion along grain boundaries of the active layer. Very good agreement between calculated and experimental data were therefore obtained for realistic kinetic parameters, $WS \times nFk \sim 15 \times 10^{-3} \text{ A cm}^{-2}$ and $b = 0.085 \text{ V dec}^{-1}$. The only problem of this model, although not as serious as an underestimation of the actual catalyst utilization, is that the effective diffusion coefficient (D) no longer has a clear physical meaning. It stands for oxygen diffusion both through sub-micrometric gas pores (the grain boundaries), and within the recast Nafion[®] phase.

4.2. Agglomerate model

As shown in Section 4.1., gas pores must exist, although cathode 2 is very thin and contains no PTFE. In our opinion, the agglomerate model is therefore more suitable for simulation of real active layers of PEFC. As a main advantage, the parameters have all a clear physical meaning and most of them can be

derived from experimental data. On the other hand, an arbitrary local geometry has to be chosen for the electrode. Hence, the agglomerate size and the macroporosity are adjusting model parameters [5]. According to the chosen model geometry, see Fig. 2(b), gas pores are simulated by crevices with a micrometric depth and a sub-micrometric width. Such small crevices may be created either by PTFE (cf. cathode 1), or during the cast process of Nafion[®] (cf. the preparation method of cathode 2). In contrast to previous works [8, 9], the existence of a thin film of pure electrolyte surrounding the agglomerates is not assumed. A simplified model geometry with only few parameters is though adequate to determine of the main limiting factors.

In Fig. 4 are displayed j and ε against E curves calculated using the agglomerate model. The best fits are obtained with the sets of adjusting parameters listed in Table 1. These results nevertheless require further discussion:

- (i) The calculated macroporosity, $\beta = 0.4$, seems consistent with the amount of PTFE within cathode 1. A suspiciously high macroporosity, $\beta = 0.5$, was firstly generated by the computer for cathode 2. An overestimation of the ionic conductivity was therefore suspected. As a result, a diminution of σ_b , by a factor of 3, yielded a good fit with $\beta = 0.1$, in agreement with the fact that cathode 2 contains no PTFE. This decrease in the bulk ionic conductivity may be physically explained by a low degree of humidity

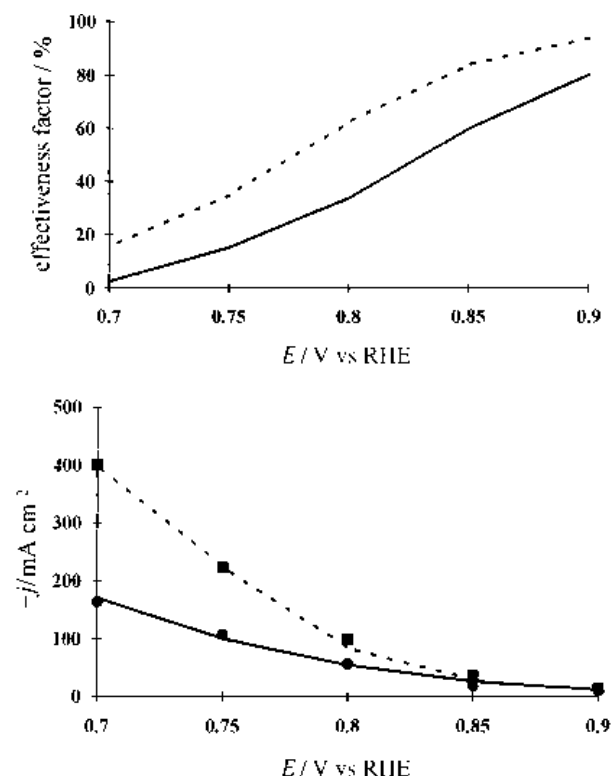


Fig. 4. Polarization characteristic [1, 2] of cathode 1 (circles) and cathode 2 (squares) fitted using the agglomerate model. The parameters (fixed or adjusted) are given in Table 1.

within the Nafion[®] phase, caused by the high operating temperature of cathode 2.

- (ii) Although the agglomerate size cannot be measured experimentally, the computer generated values agrees with the condition $a \ll L$. In addition, since small agglomerate sizes correspond to a low limitation by diffusion (cf. Appendix), simulation shows that the transport of oxygen to the catalytic sites is rather fast for cathode 2. This can be explained by homogeneous distribution of electrolyte and the coverage of each Pt particle by a very thin film of Nafion[®]. The favourable local geometry, thus obtained, may result from a previous mixing of the Pt/C powder with Nafion[®] solution (in contrast, cathode 1 is afterwards coated, which yields a less homogeneous distribution of electrolyte within the porous electrode). The effect of a large variation (from 1.5 to 0.4 μm) of the agglomerate size on the catalyst utilization is demonstrated in Fig. 4. ε decreases with E much slowly in the case of cathode 2, despite of a faster rate of charge transfer, and of a lower ionic conductivity (both related to a higher FC operating temperature than cathode 1).
- (iii) Increase of the rate of charge transfer with temperature is simulated by $\Gamma = 3$ and 6 at 50 °C and 80 °C, respectively. Similar augmentation of the catalytic activity was calculated [7], also from active layer modelling. The corresponding activation energy is about 35 kJ mol⁻¹, in agreement with measurements at the bulk Pt/TMSA interface (~ 43 kJ mol⁻¹) [22]. In contrast, an activation energy about two times greater was experimentally measured at carbon supported Pt/Nafion[®] interfaces [23]. This large discrepancy emphasizes the difficulty of direct measurements of ORR kinetics using real FC porous electrodes [23], and therefore the need of modelling.

The curves displayed in Fig. 5, show the variations of the catalyst utilization caused by modifications of the ionic conductivity along the layer thickness and/or the O₂ depth penetration within the agglomerates. The parameters σ and a varies while all the other parameters have the same values as for cathode 2. Rather small variations of the ionic conductivity significantly shift the catalyst utilization over a wide potential range (0.9 V > E > 0.7 V). At a value of σ close to that expected from room temperature measurements (curve c), the effectiveness factor is about 100%, providing that $E > 0.85$ V. Variation of the parameter a poorly modifies the catalyst utilization. This suggests, in this range of agglomerate size, a low limitation by diffusion. Nevertheless, at $E = 0.7$ V, the effectiveness factor gains about 10% as the parameter a is divided by 4 (curves a and b). This may appear modest but, in fact, corresponds to a significant increase for the current density, about 200 mA cm⁻² and better.

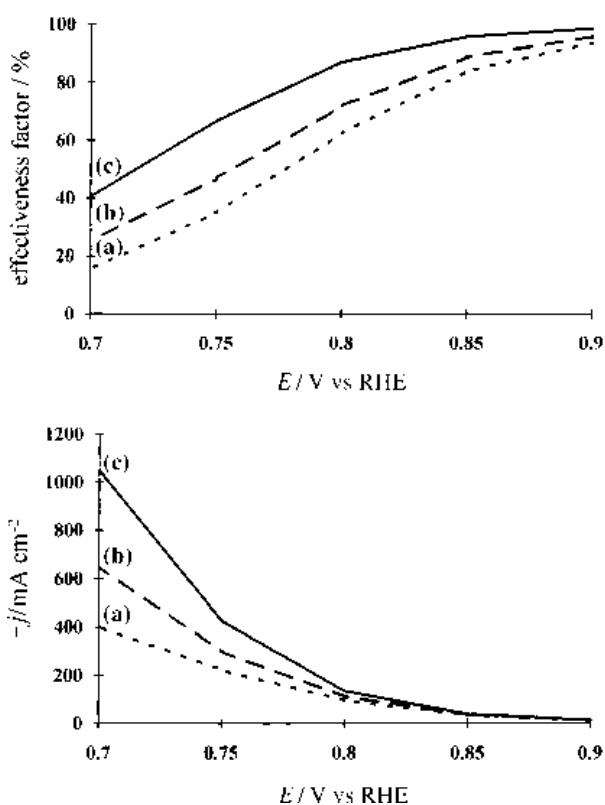


Fig. 5. Simulated curves obtained using the agglomerate model. Effectiveness factor (ε) and current density (j) are plotted against cathode potential (E). (a) base-case conditions for cathode 2, (b) $a = 0.1 \mu\text{m}$, (c) $\sigma_b = 0.05 \text{ S cm}^{-1}$.

5. Conclusion

Limitation by oxygen transport is obviously overestimated using the macrohomogeneous model. As a result, the calculated effectiveness factor is very low, and excessively high rates of charge transfer are required in the course of fitting. This suggests that oxygen diffuses not only within the electrolyte, but also through gas pores.

The agglomerate model therefore seems more suitable to simulate the operation mechanism of real PEFC active layers. In this paper, efforts are made to simplify the agglomerate geometry and thus to reduce the number of adjusting parameters. Two very different kinds of active layers (containing or not PTFE) are accurately simulated with experimentally measured kinetic and transport parameters, and with consistent sets of adjusting model parameters. This capability provides confidence in the validity of the chosen model geometry, as well as in the determination of the limiting factors.

Simulations show that the cathode performance is significantly affected by the diffusion through the agglomerate and by the ionic conduction along the layer thickness. A large decrease in the average agglomerate size can be actually obtained by mixing the Pt/C powder with Nafion[®] solution prior to constructing the active layer. The limitation by diffusion is thus reduced, enhancing notably the cathode performances at high overpotentials. On the other hand, once small agglomerates are achieved, efforts to

maintain a sufficient degree of humidity within the Nafion[®] phase seems to be particularly worthwhile. A drop in the ionic conductivity leads to a dramatic decrease in the Pt utilization and, thus, of the cathode performances, over a wide range of potentials.

References

- [1] E. A. Ticianelli, C. R. Derouin, A. Redondo and S. Srinivasan, *J. Electrochem. Soc.* **135** (1988) 2209.
- [2] M.S. Wilson and S. Gottesfeld, *ibid.* **139** (1992) L28.
- [3] S. Srinivasan, H. D. Hurwitz and J. O'M. Bockris., *J. Chem. Phys.* **46** (1967) 3108.
- [4] S. Srinivasan and H.D. Hurwitz, *Electrochim. Acta* **12** (1967) 495.
- [5] J. Giner and C. Hunter, *J. Electrochem. Soc.* **116** (1969) 1124.
- [6] D. M. Bernardi and M. W. Verbrugge, *J. Electrochem. Soc.* **139** (1992) 2477.
- [7] T. E. Springer, M. S. Wilson and S. Gottesfeld, *J. Electrochem. Soc.* **140** (1993) 3513.
- [8] T. E. Springer and I. D. Raistrick, *ibid.* **139** (1989) 1594.
- [9] E. A. Ticianelli, *J. Electroanal. Chem.* **387** (1995) 1.
- [10] P. Stonehart and P. Ross, *Electrochim. Acta* **21** (1976) 441.
- [11] R. E. Meredith and C. W. Tobias, in 'Advances in Electrochemistry and Electrochemical Engineering', Vol.2 (edited by C.W. Tobias), Interscience, New York (1962), p.15.
- [12] F. Gloaguen, F. Andolfatto, R. Durand and P. Ozil, *J. Appl. Electrochem.* **24** (1994) 863.
- [13] S. Gottesfeld, I. D. Raistrick and S. Srinivasan, *J. Electrochem. Soc.* **134** (1987) 1455.
- [14] W. Paik, T. E. Springer and S. Srinivasan. *ibid.* **136** (1989) 644.
- [15] A. Parthasarathy, C. R. Martin and S. Srinivasan, *ibid.* **138** (1991) 916.
- [16] F. A. Uribe, T. E. Springer and S. Gottesfeld, *ibid.* **139** (1992) 765.
- [17] A. Parthasarathy, S. Srinivasan, A. J. Appleby and C. R. Martin, *ibid.* **139** (1992) 2858.
- [18] K. Kinoshita, *ibid.* **137** (1990) 845.
- [19] A. Kabbabi, F. Gloaguen, F. Andolfatto and R. Durand, *J. Electroanal. Chem.* **373** (1994) 251.
- [20] Z. Ogumi, Z. Takehara and S. Yoshizawa, *J. Electrochem. Soc.* **131** (1984) 769.
- [21] S. Gottesfeld, *ibid.* **139** (1992) 2980.
- [22] A. J. Appleby and B. S. Baker, *ibid.* **125** (1978) 404.
- [23] A. Parthasarathy, S. Srinivasan, A. J. Appleby and C. R. Martin, *J. Electroanal. Chem.* **339** (1992) 101.
- [24] R. P. Ickowski and M. B. Cutlip, *J. Electrochem. Soc.* **127** (1980) 1433.
- [25] E. Fontes, C. Lagergren and D. Simonsson, *Electrochim. Acta.* **38** (1993) 2669.
- [26] Y. Sone, P. Ekdunge and D. Simonsson, *J. Electrochem. Soc.* **143** (1996) 1254.

Appendix

(a) The macrohomogeneous model has been accurately described elsewhere [6, 7]. Both oxygen diffusion and ionic conduction occur along the layer thickness (the x axis, see Fig. 2(a)). Using the Fick's law and the Ohm's law to describe the distribution of concentration (c) and of overpotential (η), respectively

$$\eta(L) - \eta(0) = -\frac{L}{\sigma}j + \frac{nFD}{\sigma}[c_b - c(L)] \quad (\text{A1})$$

$c(L) = c_b$ yields $\eta(L) - \eta(0) = L_j/\sigma$, the maximum in absolute value for ohmic drop. In the case of cathode 2, j is about -400 mA cm^{-2} for $\eta(L) = E - 0.9 = -0.2 \text{ V}$ (E being the measured cathode potential),

and thus $|L_j/\sigma| \sim 0.02 \text{ V}$. This means that the limitation by ohmic drop can be roughly neglected for $|\eta(L)| < 0.2 \text{ V}$. Nevertheless, at higher overpotentials and/or for a very accurate simulation, the ohmic drop should be accounted for as described elsewhere [7]. For a low limitation by ohmic drop, the effectiveness factor (ε) is calculated by [12]

$$\varepsilon = \frac{\tanh\left[u e^{-2.3\eta(L)/b}\right]^{1/2}}{\left[u e^{-2.3\eta(L)/b}\right]^{1/2}} \quad \text{with } u = \frac{\Gamma n F k \gamma L^2}{n F D c_b} \quad (\text{A2})$$

and the total current density is obtained by

$$j = \varepsilon \times W S i^* = -\varepsilon \times W S \times n F k e^{-2.3\eta(L)/b}$$

ε and j are thus calculated for given values of $\eta(L)$ and u , which is a function of the key parameters that characterize the active layer (Fig. 3).

(b) The agglomerate model was firstly introduced by Giner and Hunter [5], and after that developed by several authors [e.g., 8, 9, 24, 25]. In our simulations, the agglomerate have a slab geometry of $L \times 2a \times 1 \text{ cm}^3$ (see Fig. 2(b)). Since $a \ll L$, the oxygen diffusion occurs mainly along the agglomerate width (the y axis). In a differential element dx of one agglomerate, the simultaneous transport and consumption of protons and oxygen, along the y axis, is expressed by [8]

$$\eta(0) - \eta(a) = \frac{nFD}{\sigma}[c_b - c(0)] \quad (\text{A3})$$

$c(0) = 0$ yields $\eta(0) - \eta(a) \sim 10^{-4} \text{ V}$. This means that the ohmic drop along the y axis is almost negligible. Hence, the overpotential varies only along the x axis, as follows:

$$I_2(x) = -(2 \times 1)nFD \int_0^x \left(\frac{dc}{dy}\right)_a dx = (2a \times 1)\sigma \frac{d\eta}{dx} \quad (\text{A4})$$

where $I_2(x)$ is the ionic current along one agglomerate of cross-section $(2a \times 1) \text{ cm}^{-2}$. The boundary conditions of Equation A4 are $I_2(0) = 0$ and $I_2(L) = I$, I being the total current generated by one agglomerate at $\eta(L)$. By analogy with the work reported by Giner *et al.* [5], the overpotential distribution along the agglomerate length is given by

$$\frac{d^2H}{dX^2} = \frac{v}{u'} \left(u' e^H\right)^{1/2} \tanh\left(u' e^H\right)^{1/2} \quad (\text{A5})$$

with $u' = \Gamma n F k \gamma a^2 / n F D c_b$ and $v = 2.3 \Gamma n F k \gamma L^2 / b \sigma$ and where $X = x/L$ and $H = -2.3\eta/b$.

The boundary conditions of Equation A5 are $(dH/dX)_0 = 0$ and $H(1) = -2.3\eta(L)/b$. Equation A5 must be solved numerically. The Runge-Kutta method is used to calculate the overpotential distribution, but several iterations are needed to find the value of H at $x = 0$ for which $H(1) = -2.3\eta(L)/b$. We are then able to calculate I and thus the effectiveness factor as follows:

$$\varepsilon = \frac{(dH/dX)_1}{v e^{H(1)}} \quad (\text{A6})$$

Within a differential element dx , the depth utilization of the catalyst is characterized by the product $[ue^{H(1)}]^{1/2}$ in Equation A5. For $[ue^{H(1)}]^{1/2} < 0.5$, $\tanh [ue^{H(1)}]^{1/2} \sim [ue^{H(1)}]^{1/2}$, and Equation A5 becomes: $d^2H/dX^2 = \bar{v}e^H$. This equation describes the operation mechanism of an active layer controlled by the ohmic drop and the charge transfer (the limitation by

diffusion being negligible) [12]. The condition $[ue^{H(1)}]^{1/2} < 0.5$ is satisfied for $a < 0.3 \mu\text{m}$ and $|\eta(L)| < 0.25 \text{ V}$. This result emphasizes that when the agglomerate size is not too large (as in the case of the cathode 2), limitation by diffusion occurs mainly at high overpotential. In contrast, a significant limitation by ohmic drop occurs at any overpotential.